

LETTERS

The recent formation of Saturn's moonlets from viscous spreading of the main rings

Sébastien Charnoz¹, Julien Salmon¹ & Aurélien Crida^{2,3}

The regular satellites of the giant planets are believed to have finished their accretion concurrent with the planets, about 4.5 Gyr ago^{1–4}. A population of Saturn's small moons orbiting just outside the main rings are dynamically young^{5,6} (less than 10⁷ yr old), which is inconsistent with the formation timescale for the regular satellites. They are also underdense⁷ (~600 kg m⁻³) and show spectral characteristics similar to those of the main rings^{8,9}. It has been suggested that they accreted at the rings' edge^{7,10,11}, but hitherto it has been impossible to model the formation process fully owing to a lack of computational power. Here we report a hybrid simulation in which the viscous spreading of Saturn's rings beyond the Roche limit (the distance beyond which the rings are gravitationally unstable) gives rise to the small moons. The moonlets' mass distribution and orbital architecture are reproduced. The current confinement of the main rings and the existence of the dusty F ring are shown to be direct consequences of the coupling of viscous evolution and satellite formation. Saturn's rings, like a mini protoplanetary disk, may be the last place where accretion was recently active in the Solar System, some 10⁶–10⁷ yr ago.

The low density of Saturn's small moons and their icy composition, closeness to the rings and rapid tidal timescales have long suggested that their origin may be linked to the planet's icy rings. On the one hand, the population of small moons exterior to the Roche limit (Atlas, Prometheus, Pandora, Janus and Epimetheus) have a mass–distance relation remarkably different from Saturn's main satellites (Fig. 1). On the other hand, *N*-body simulations^{10,12} show that ring material spreading viscously beyond 142,000 km (measured from Saturn's centre) would be gravitationally unstable and that ~100-m aggregates would form in less than ten orbits. Below 138,000 km, accretion becomes inefficient^{12–14}, so the outer edge of the region in which accretion is prevented (the 'Roche region') is at $R_L \approx 140,000 \pm 2,000$ km. This differs slightly from the classical definition of the Roche Limit because its precise location depends on a diversity of factors, such as the bodies' relative sizes, spins^{14,15} and so on. Today, the main rings' outermost region, the A ring, is sharply bounded at 136,775 km by Janus's gravitational torque^{5,16}. However, this configuration must be transient (<10 Myr) because the rings repel Janus and, in turn, are pushed inwards to conserve angular momentum. As the moon migrates outwards, the radius to which the rings' outer edge is confined changes accordingly and may pass the nearby Roche limit. Therefore, ring material may have spread beyond Saturn's Roche limit in the past, or may do so in the future.

To simulate the coupled evolution of aggregates with the rings on long timescales (~1 Gyr), we designed a hybrid model in which two codes are self-consistently coupled¹⁷: a one-dimensional hydrodynamical model to track the rings' viscous evolution and an analytical orbital model to track the aggregates. We compute the evolution of the ring's surface density, $\sigma(r)$, using a finite-element scheme, on a

staggered mesh, solving for the surface density equation of a Keplerian disk under the effect of viscous torque and moonlets' gravitational torques¹⁸:

$$\frac{d\sigma}{dt} = \frac{3}{r} \frac{\partial}{\partial r} \left[r^{1/2} \frac{\partial}{\partial r} (v(r)\sigma r^{1/2}) - \frac{1}{3\pi(GM)^{1/2}} r^{1/2} T(r) \right]$$

Here r , $v(r)$, G and M are the distance from Saturn, the local viscosity, the gravitational constant and Saturn's mass, respectively, and $T(r)$ is the sum, over all the satellites, of the local Lindblad-resonance torque densities (Supplementary Information, section 1). A realistic viscosity model, in which the viscosity is an increasing function of the surface density, is used¹⁹. Because aggregates are formed at $r \geq R_L$ after only a few orbital periods (which is negligible in comparison with the timescale of viscous spreading), the accretion of ring material into aggregates is considered to occur instantaneously: at each time step, all ring mass located beyond R_L is removed from the hydrodynamical simulation and transformed into one additional aggregate.

Each aggregate (also called a moonlet) is tracked and its mass, m_s , semi-major axis, a_s , and eccentricity, e_s , tabulated (Supplementary Information, section 2). The resultant eccentricities are so small (<10⁻⁴) that they do not influence the system's evolution. The semi-major axes evolve under the effects of Saturn's tides and ring torque according to

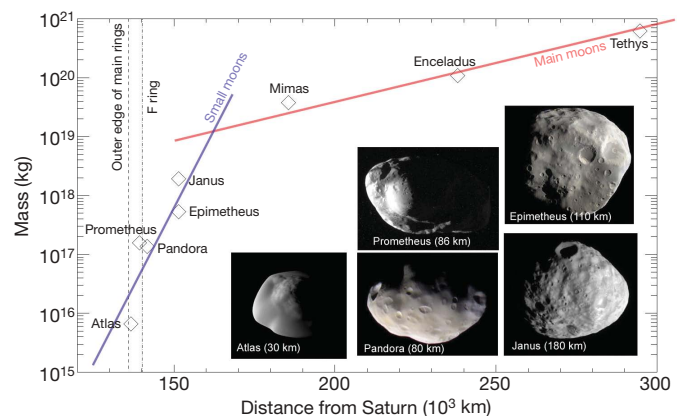


Figure 1 | Mass of Saturn's inner moons versus distance. The names and average diameters of the moons are indicated in the insets. Data for Mimas, Enceladus and Tethys are also plotted, for comparison. The vertical dashed line shows the location of the outer edge of Saturn's A ring, at 136,775 km, and the vertical dash-dot line indicates the location of the F ring (a ~1,000-km-wide ringlet located between Prometheus and Pandora). The blue and red lines show simple logarithmic fits to the mass–distance data for the small moons and, respectively, the main moons. Images from the Cassini mission (courtesy of NASA/JPL/SSI).

¹Laboratoire AIM, Université Paris Diderot/CEA/CNRS, 91191 Gif sur Yvette, France. ²Department of Applied Mathematics and Theoretical Physics, University of Cambridge, Cambridge CB3 0WA, UK. ³Université de Nice Sophia-Antipolis/CNRS/Observatoire de la Côte d'Azur, Laboratoire Cassiopée, BP4229, 06304 Nice Cedex 4, France.

$$\frac{da_s}{dt} = \frac{3k_{2p}m_sG^{1/2}R_p^5}{Q_pM^{1/2}a_s^{11/2}} + \frac{2a_s^{1/2}\Gamma_s}{m_s(GM)^{1/2}}$$

where Q_p , k_{2p} and R_p denote the planet's dissipation factor, Love number and radius, respectively (Supplementary Information, section 1.2), and Γ_s is the sum of the ring torques of all first-order Lindblad resonances of the moonlet^{6,18,20}. When the orbital separation of two moonlets is smaller than 2.2 mutual Hill radii, they are merged¹². To test the full procedure, the formation of the proto-Moon from a circumterrestrial disk was successfully reproduced²¹ (Supplementary Information, section 3).

The initial conditions are as follows. The A ring is initially represented by a disk extending from 122,000 km to 136,000 km with a constant surface density, σ_0 . The initial state of Saturn's rings is unknown and they could have been denser in the past²². We considered the cases in which $\sigma_0 = 400, 1,000, 5,000$ and $10,000 \text{ kg m}^{-2}$. The case in which $\sigma_0 = 400 \text{ kg m}^{-2}$ (approximately the present surface density of Saturn's A ring) is presented in Fig. 2 with R_L set to 140,000 km.

The simulation starts with no satellites, so the A ring initially spreads freely and reaches R_L in $\sim 10^6$ yr (Fig. 2). Then moonlets accrete at R_L from the ring material and grow through mutual encounters. They induce step-like structures in the ring's surface density near the moonlets' Lindblad resonances (Fig. 2a–d). At these locations, the ring angular momentum is directly transferred to the moonlets, inducing an orbital decay of the ring material and an expansion of the moonlets' orbit. As a consequence, the ring material moves inwards and accumulates just interior to the resonance location, resulting in the visible step-like structures in the surface density function. Whereas Γ_s increases with the moonlets' mass, the disk's surface density decreases as a result of spreading and thus so do the viscosity and the viscous torque, Γ_v (ref. 16). When the magnitude of Γ_s becomes larger than that of Γ_v , the disk's outer edge is confined and the disk stops spreading (Fig. 2e). This happens when the largest moon reaches a mass of $\sim 10^{17} \text{ kg}$ for $\sigma_0 \leq 1,000 \text{ kg m}^{-2}$ and $\sim 10^{18} \text{ kg}$ for $\sigma_0 \geq 5,000 \text{ kg m}^{-2}$. As the moonlets' masses increase, the ring's outer edge moves inwards to the position of the first

Lindblad resonance for which the torque is strong enough to counterbalance Γ_v . On long timescales, owing to the decrease of the surface density, confinement is increasingly easier, and in this model the ring's outer edge moves inwards to $\sim 135,000 \text{ km}$ after 4 Gyr for $\sigma_0 = 400 \text{ kg m}^{-2}$. For higher values of σ_0 , the disk undergoes more rapid viscous spreading and more massive moonlets are formed; this ultimately shifts the disk's edge below 130,000 km for $\sigma_0 > 1,000 \text{ kg m}^{-2}$. In conclusion, the current confinement of the outer edge of Saturn's rings seems to be the consequence of ongoing satellite accretion occurring at the Roche limit. The outer edge jumps from one resonance to another, depending on the local balance between the positive viscous torque and the negative torque induced by the population of small moons.

The moonlets migrate outwards owing to the positive torques induced by the rings and the planet. Because, for each moonlet, these torques are increasing functions of mass²⁰ ($\Gamma_s \propto m_s^2$), the migration rate increases accordingly and more massive moonlets migrate more rapidly. Different migration rates lead to crossings and merging. Because all moonlets appear at the same position (R_L), a simple orbital architecture emerges in which satellites are radially sorted: their distance to Saturn is an increasing function of their mass, in agreement with observations (Fig. 1). Therefore, the actual orbital architecture of the small moons may be the direct consequence of ring–moon interactions.

These results imply also that Saturn's small moons are gravitational aggregates made of icy ring particles, which would explain their very low densities. When they form, they should be initially elongated like Hill spheres^{7,10}, as is observed for some of the moons⁷. Pandora and Epimetheus seem to deviate somewhat from this shape⁷, but this could result from post-accretional restructuring. The moons' spectral similarities with Saturn's rings^{9,23} may be the direct result of their formation within the rings, as might be their apparent lack of silicates⁷, as Saturn's rings seem to be devoid of such material^{18,23}.

The coupling of ring confinement with moonlet migration induces a feedback on the formation rate of the moonlets. When the ring's edge is repelled to below R_L , the production of moonlets stops (compare

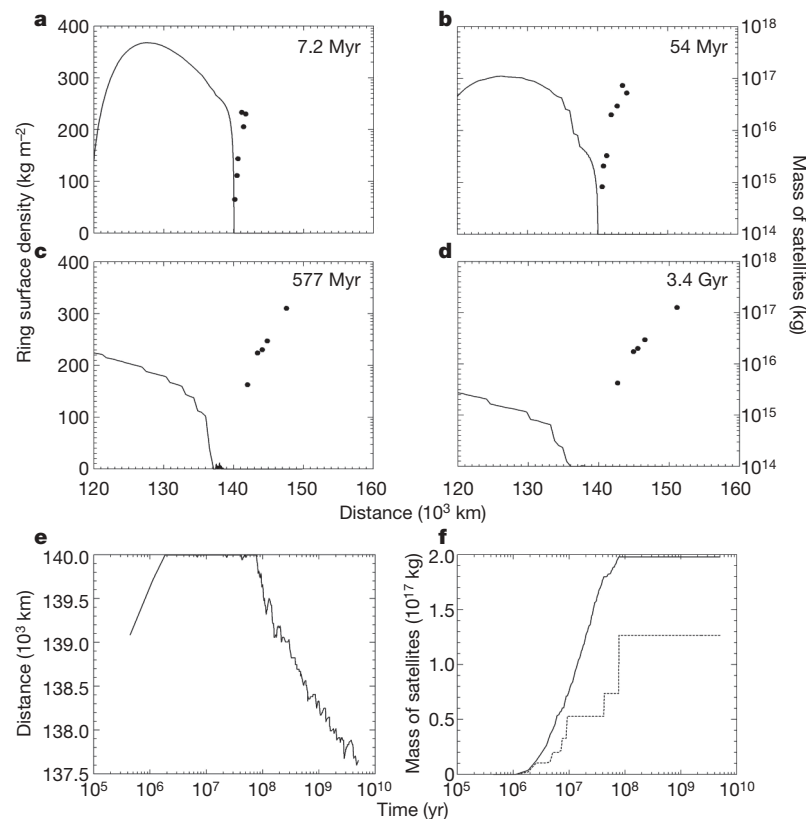


Figure 2 | Time evolution of our model with $\sigma_0 = 400 \text{ kg m}^{-2}$. a–d, The time evolution of the ring's surface density (solid line) and the masses of the moonlets (black points) as functions of the distance from Saturn's centre. As the ring spreads inwards and outwards, its surface density decreases. Ring material crossing the Roche limit ($R_L = 140,000 \text{ km}$ here) is transformed into moonlets. At the end of the simulation, only $1.5 \times 10^{18} \text{ kg}$ of the ring material remains in the A ring, whereas $3.5 \times 10^{18} \text{ kg}$ is spread below 120,000 km and $1.8 \times 10^{17} \text{ kg}$ has been transformed into moonlets. e, The time evolution of the location of the ring's outer edge, defined as the place where the surface density drops below 1 kg m^{-2} . When the edge is confined at the location of a moonlet's resonance, the ring's viscous torque (which tends to push material beyond the ring's edge by transferring angular momentum) is perfectly balanced by the satellite's gravitational torque, thus preventing the ring material from spreading farther outwards. f, Total mass transformed into satellites as a function of time. The dashed line shows the mass of the largest satellite.

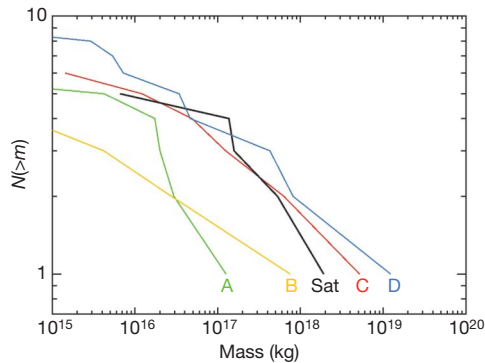


Figure 3 | Comparing the mass distribution of the moonlets obtained in our simulation with observations. Cumulative mass distributions of moonlets obtained in four simulations with different initial surface densities, fitted with single power-law functions of the form $N(>m) \propto m^{-\alpha}$; case A ($\sigma_0 = 400 \text{ kg m}^{-2}$, $\alpha = 0.31 \pm 0.06$; case B ($\sigma_0 = 1,000 \text{ kg m}^{-2}$, $\alpha = 0.19 \pm 0.01$; case C ($\sigma_0 = 5,000 \text{ kg m}^{-2}$, $\alpha = 0.22 \pm 0.03$; case D ($\sigma_0 = 10,000 \text{ kg m}^{-2}$, $\alpha = 0.17 \pm 0.04$). The actual population of Saturn's moonlets (Sat, $\alpha = 0.27 \pm 0.07$) is well within the range of masses and number of bodies obtained in the simulations. We note that some of our distributions (A, B and C) show a knee and a shallower slope at smaller sizes, as is observed for Saturn's small moons (Sat).

Fig. 2e and Fig. 2f). Conversely, as moonlets move away from the planet, the location of the ring's edge follows and satellite production can set in again for any ring material that reaches R_L . This stop-and-go mechanism is apparent in the mass history of the satellites (Fig. 2f): it limits their mass to about the smallest mass necessary to confine the ring and can be analytically estimated (Supplementary Information, section 4). The mass distributions of moonlets obtained in our simulations well match the observed distribution, having a similar logarithmic exponent and overall shape (Fig. 3). However, these results may be affected by nonlinearities that could arise in the torques of the most massive satellites (Supplementary Information, section 3.4). A direct consequence of this feedback mechanism is that the mass of the largest moon must be of the order of the mass necessary to confine the ring: this is actually the case with Janus, the most massive of the small moons, which confines the A ring's outer edge^{5,16}. The current mass of Janus implies that the A ring surface density was between $1,000 \text{ kg m}^{-2}$ and $5,000 \text{ kg m}^{-2}$ at the time Janus formed (whereas the ring's total mass remains undetermined²⁴).

Saturn's main rings are encircled by a dusty and dynamically active ringlet, called the F ring, which is located 140,500 km from Saturn's centre and whose origin is still debated. In the present work, its presence may have a simple explanation: owing to the spreading of the A ring, aggregates are formed at $\sim 140,000 \text{ km}$ and suffer subsequent collisional evolution while migrating outwards. Because accretion should not be 100% efficient below 142,000 km (ref. 14), colliding aggregates will release dust and produce a dusty ring with a non-negligible mass, like today's F ring^{25–27}. In the current orbital configuration, the F ring is not provided with new aggregates from the A ring because of the confinement induced by Janus. However, on longer timescales, the dusty F ring will again be supplied with mass when the A ring again viscously spreads. Thus, the F ring should have always been present because of the regular renewal of its material. In this picture, it is considered to be the dusty signature of ring material crossing the Roche limit as a result of the global viscous spreading of the rings. The F-ring material should be about the same age as the nearby moonlets²⁵, 10^6 – 10^7 yr, although the main rings could be older.

Received 15 December 2009; accepted 15 April 2010.

1. Mosqueira, I. & Estrada, P. R. Formation of the regular satellites of giant planets in an extended gaseous nebula I: subnebula model and accretion of satellites. *Icarus* **163**, 198–231 (2003).
2. Canup, R. & Ward, W. R. Formation of the Galilean satellites: conditions for accretion. *Astron. J.* **124**, 3404–3423 (2002).
3. Canup, R. M. & Ward, W. R. A common mass scaling for satellite systems of gaseous planets. *Nature* **411**, 834–839 (2006).
4. Estrada, P. R., Mosqueira, I., Lissauer, J. J., D'Angelo, G. & Cruikshank, D. P. in *Europa* (eds McKinnon, W., Pappalardo, R. & Khurana, K.) 27–58 (Univ. Arizona Press, 2009).
5. Lissauer, J. J. & Cuzzi, J. N. Resonances in Saturn's rings. *Astron. J.* **87**, 1051–1058 (1982).
6. Poulet, F. & Sicardy, B. Dynamical evolution of the Prometheus-Pandora system. *Mon. Not. R. Astron. Soc.* **322**, 343–355 (2001).
7. Porco, C. C., Thomas, P. C., Weiss, J. W. & Richardson, D. C. Physical characteristics of Saturn's small satellites provide clues to their origins. *Science* **318**, 1602–1607 (2007).
8. Poulet, F., Cruikshank, D. P., Cuzzi, J. N., Roush, T. L. & French, R. G. Compositions of Saturn's rings A, B, and C from high resolution near-infrared spectroscopic observations. *Astron. Astrophys.* **412**, 305–316 (2003).
9. Coradini, A. et al. Saturn satellites as seen by Cassini mission. *Earth Moon Planets* **105**, 289–310 (2009).
10. Karjalainen, R. & Salo, H. Gravitational accretion of particles in Saturn's rings. *Icarus* **172**, 328–348 (2004).
11. Charnoz, S., Brahic, A., Thomas, P. & Porco, C. The equatorial ridges of Pan and Atlas: late accretionary ornaments? *Science* **318**, 1622–1624 (2007).
12. Karjalainen, R. Aggregate impacts in Saturn's rings. *Icarus* **189**, 523–537 (2007).
13. Ohtsuki, K. Capture probability of colliding planetesimals: dynamical constraints on accretion of planets, satellites, and ring particles. *Icarus* **106**, 228–246 (1993).
14. Canup, R. M. & Esposito, L. W. Accretion in the Roche zone: coexistence of rings and ring moons. *Icarus* **113**, 331–352 (1995).
15. Weidenschilling, S. J., Chapman, C. R., Davis, D. R. & Greenberg, R. in *Planetary Rings* (eds Greenberg, R. & Brahic, A.) 367–415 (Univ. Arizona Press (1984).
16. Spitale, J. N. & Porco, C. C. Time variability in the outer edge of Saturn's A-ring revealed by Cassini imaging. *Astron. J.* **138**, 1520–1528 (2009).
17. Salmon, J., Charnoz, S. & Crida, A. Long-term and large scale simulation of Saturn's rings viscous evolution. *Icarus* (in the press).
18. Takeuchi, T., Miyama, S. M. & Lin, D. N. C. Gap formation in protoplanetary disks. *Astrophys. J.* **460**, 832–847 (1996).
19. Daisaka, H., Tanaka, H. & Ida, S. Viscosity in a dense planetary ring with self-gravitating particles. *Icarus* **154**, 296–312 (2001).
20. Meyer-Vernet, N. & Sicardy, B. On the physics of resonant disk-satellite interaction. *Icarus* **69**, 157–175 (1987).
21. Kokubo, E., Ida, S. & Makino, J. Evolution of a circumterrestrial disk and formation of a single moon. *Icarus* **148**, 419–436 (2000).
22. Charnoz, S., Morbidelli, A., Dones, J. & Salmon, A. Did Saturn's rings form during the Late Heavy Bombardment? *Icarus* **199**, 413–428 (2009).
23. Cuzzi, J. et al. in *Saturn from Cassini-Huygens* (eds Dougherty, M. K., Esposito, L. W. & Krimigis, T.) 535–573 (Springer, 2009).
24. Charnoz, S., Dones, L., Esposito, L. W., Estrada, P. R. & Hedman, M. M. in *Saturn from Cassini-Huygens* (eds Dougherty, M. K., Esposito, L. W. & Krimigis, T.) 459–509 (Springer, 2009).
25. Murray, C. D. et al. The determination of the structure of Saturn's F ring by nearby moonlets. *Nature* **453**, 739–744 (2008).
26. Showalter, M. R., Pollack, J. B., Ockert, M. B., Doyle, L. R. & Dalton, J. B. A photometric study of Saturn's F ring. *Icarus* **100**, 394–411 (1992).
27. Charnoz, S. Physical collisions of moonlets and clumps with the Saturn's F ring core. *Icarus* **201**, 191–197 (2009).

Supplementary Information is linked to the online version of the paper at www.nature.com/nature.

Acknowledgements This work was funded by Université Paris Diderot and CEA/IRFU/SAP. The authors thank F. Bournaud, J. Burns, L. Dones, Z. Leinhardt and H. Throop.

Author Contributions S.C. and J.S. designed the code and analysed the results, and A.C. was involved in the analysis of the results and provided critical contributions.

Author Information Reprints and permissions information is available at www.nature.com/reprints. The authors declare no competing financial interests. Readers are welcome to comment on the online version of this article at www.nature.com/nature. Correspondence and requests for materials should be addressed to S.C. (charnoz@cea.fr).